MILLIMETER-WAVELENGTH RADARS New Frontier in Atmospheric Cloud and Precipitation Research

BY P. KOLLIAS, E. E. CLOTHIAUX, M. A. MILLER, B. A. ALBRECHT,
G. L. STEPHENS, AND T. P. ACKERMAN

Millimeter-wavelength radars bridge an observational gap in Earth's hydrological cycle by adequately detecting clouds and precipitation, thus offering a unique and more holistic view of the water cycle in action.

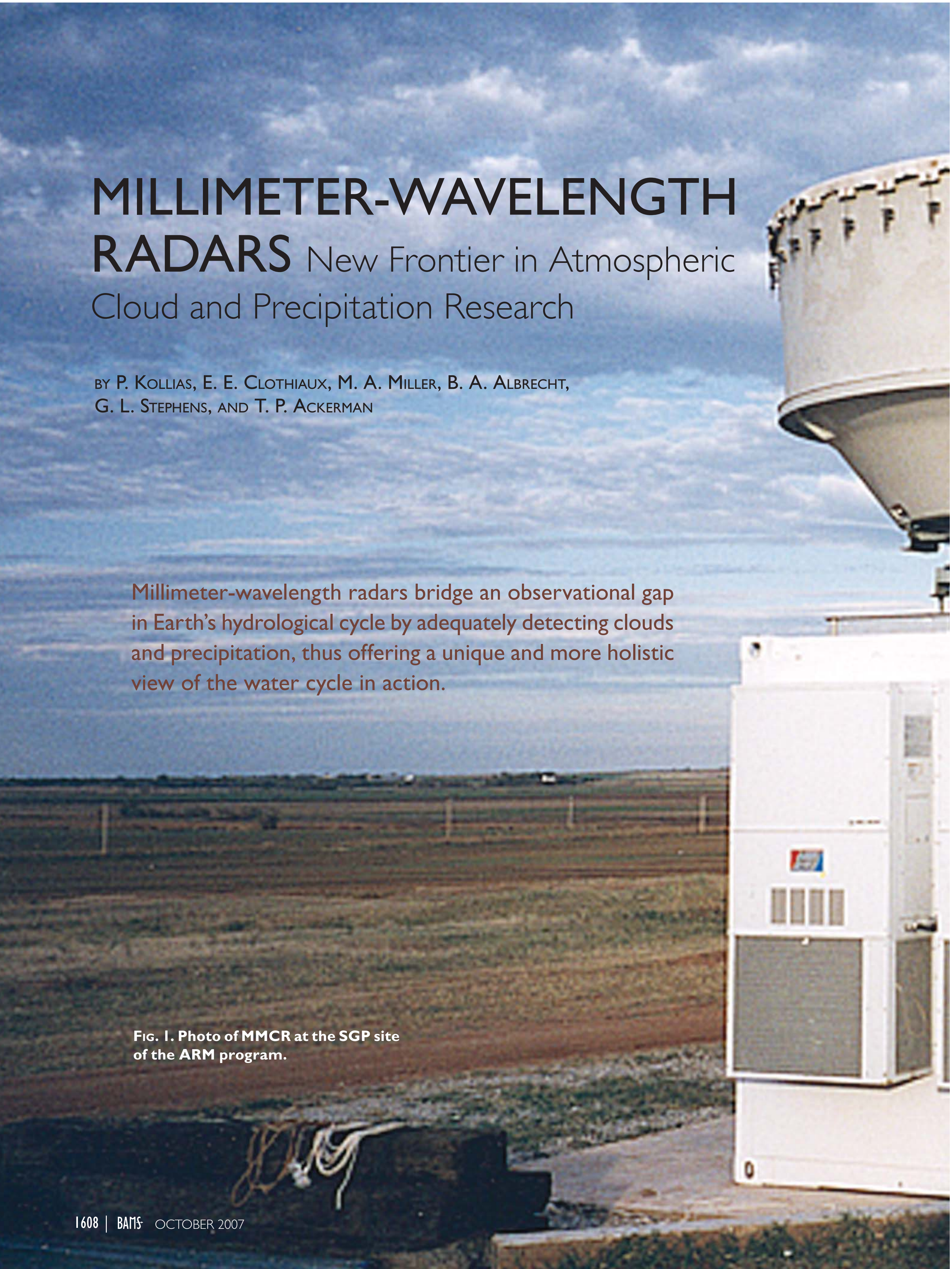

FIG. 1. Photo of MMCR at the SGP site of the ARM program.

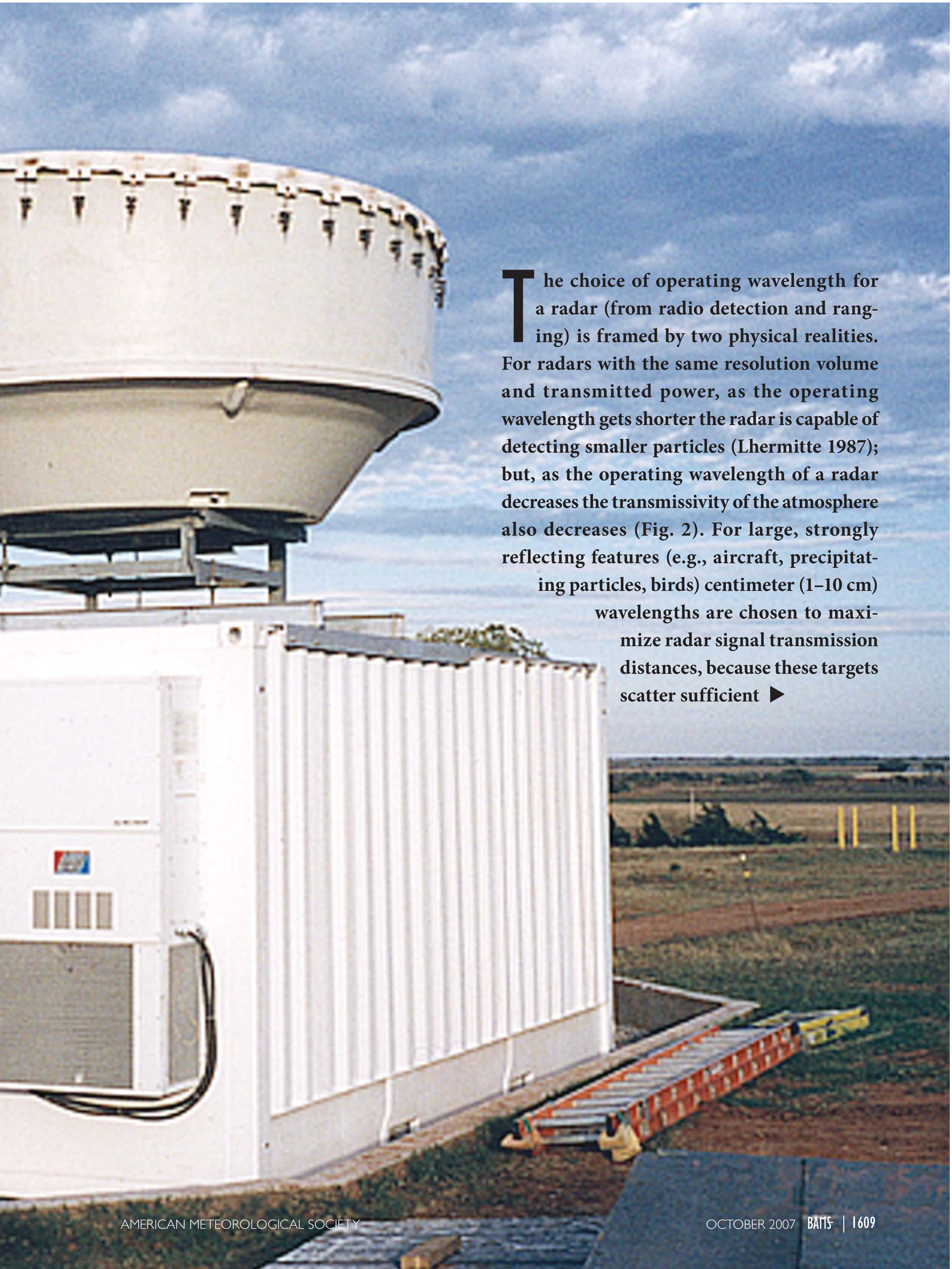

The choice of operating wavelength for a radar (from radio detection and ranging) is framed by two physical realities. For radars with the same resolution volume and transmitted power, as the operating wavelength gets shorter the radar is capable of detecting smaller particles (Lhermitte 1987); but, as the operating wavelength of a radar decreases the transmissivity of the atmosphere also decreases (Fig. 2). For large, strongly reflecting features (e.g., aircraft, precipitating particles, birds) centimeter (1–10 cm) wavelengths are chosen to maximize radar signal transmission distances, because these targets scatter sufficient ▶

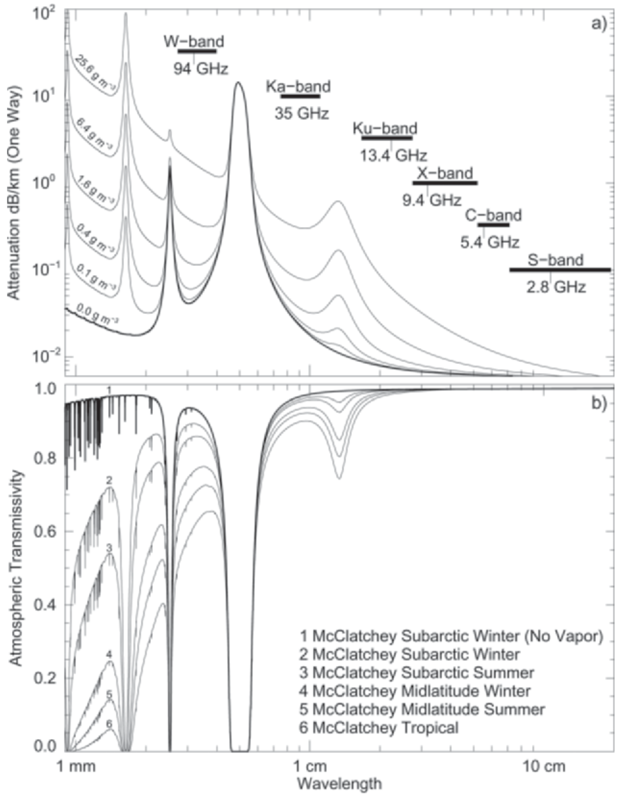

Fig. 2. Atmospheric transmissivity versus wavelength for (a) a 1-km horizontal path at the surface with a pressure of 1010 mb, a temperature of 294 K, and water vapor amounts varying from 0 to 26.6 g m^{-3}, and (b) vertical paths from the surface to space (i.e., 100 km of altitude) through the McClatchey et al. (1972) subarctic winter and summer, midlatitude summer and winter, and tropical profiles. Transmissivities for the 0 g m^{-3} curve in (a) and the McClatchey subarctic winter profile with no water vapor in (b) illustrate the drop in transmission resulting from molecular oxygen (O_2) absorption. The remaining curves illustrate the increased losses in transmission with increasing amounts of atmospheric water vapor. The transmissivities in (a) are reported in decibels per kilometer, or $-10 \log_{10}(t_{1\ km})$, where $t_{1\ km}$ is the transmissivity along the 1-km horizontal path. All of these transmissivities were calculated with the Monochromatic Radiative Transfer Model (MonoRTM; Delamere et al. 2002), developed by Tony Clough at Atmospheric and Environmental Research (AER), Inc.

power back to the radar to be detected over hundreds of kilometers from the radar. Cloud particles with diameters in the range from 5 to 10 μm are most often too small to be detected by centimeter-wavelength radars. To detect cloud particles reliably, shorter millimeter-wavelength radars are necessary. However, the drop in atmospheric transmissivity from centimeter to millimeter wavelengths limits the range of millimeter-wavelength radars. In precipitation-free conditions a range of tens of kilometers is possible, but with the onset of precipitation the useful observation range decreases.

Millimeter-wavelength radars complement the popular and widely used centimeter-wavelength radars (e.g., National Weather Service radars and television station radars), of which the general public is most aware, in that in addition to precipitation storms, they are also capable of detecting nonprecipitating clouds. Clouds have a profound impact on the Earth's climate. Their study has become a topic of great interest during the past 20–30 yr and millimeter-wavelength (cloud) radars have emerged as an important tool in characterizing their properties. Cloud radars are now being used in conjunction with lidar systems—one of the principal tools from the 1980s—in the study of clouds, including thin cirrus. Because of their short wavelengths, cloud radars have excellent sensitivity to small cloud droplets and ice crystals, can be configured to have high temporal and spatial resolutions, and can operate with antennas that have narrow beamwidths and limited sidelobes (Clothiaux et al. 1995; Kropfli and Kelly 1996; Lhermitte 1990). Their portability and compact size make them a powerful research tool that can be deployed on various platforms, including ships, aircraft, and satellites.

We briefly discuss millimeter-wavelength radar developments from the 1980s through the present. [Earlier reviews on the use and application of cloud radars can be found in Mead et al. (1994) and

AFFILIATIONS: Kollias—Department of Atmospheric and Oceanic Sciences, McGill University, Montreal, Quebec; Clothiaux—Department of Meteorology, The Pennsylvania State University, University Park, Pennsylvania; Miller—Department of Environmental Sciences, Rutgers University, New Brunswick, New Jersey; Albrecht—Division of Meteorology and Physical Oceanography, University of Miami, Miami, Florida; Stephens—Department of Atmospheric Science, Colorado State University, Fort Collins, Colorado; Ackerman—Department of Atmospheric Sciences, University of Washington, Seattle, Washington
CORRESPONDING AUTHOR: Dr. Pavlos Kollias, Department of Atmospheric and Oceanic Sciences, McGill University, 805 Sherbrooke Street West, Montreal, Quebec, H3A 2K6 Canada
E-mail: pavlos.kollias@mcgill.ca

The abstract for this article can be found in this issue, following the table of contents.
DOI:10.1175/BAMS-88-10-1608

In final form 12 January 2007

Kropfli and Kelly (1996).] We then focus on the nature of millimeter-wavelength radar data as they exist today, and the range of applications to which these data can be applied. Polarimetric applications of cloud radars are not discussed. Last, we look to the future and plan for advanced applications of millimeter-wavelength radars, as well as new cloud and precipitation research applications based on even higher-frequency radars.

HISTORICAL OVERVIEW OF CLOUD RADAR DEVELOPMENT. The use of radars for meteorological applications originated soon after the end of World War II. Early on, the military was bothered by the presence of clusters of precipitation echoes on radar analog plan position indicator (PPI) displays that distracted from their efforts to detect approaching airplanes. But, one person's noise is another's signal. Meteorologists understood the potential of radars for the detection and study of precipitation over large ranges. Using available military surplus, in the 1950s they developed the first meteorological radars operating at centimeter (1–10 cm) wavelengths. A description of the early days in radar meteorology can be found in Atlas (1990), Rogers and Smith (1996), Lhermitte (2002), and Brown and Lewis (2005).

The first efforts to develop short-wavelength radars were carried out by the U.S. Air Force and can also be traced back to the years just after World War II. The first use of shorter-wavelength radars for cloud observations was made in the 1950s using 1.2-cm-wavelength radars (Plank et al. 1955). In the 1960s, the U.S. Air Force developed the AN/TPQ-11, a high-power 35-GHz system originally assigned to cloud-deck monitoring near airports, as a replacement for the ceilometer (Table 1). A large number of these systems were developed—more cloud radars were built in the 1960s than any other decade—and a number of studies (e.g., Petrocchi and Paulsen 1966; Paulsen et al. 1970) demonstrated that these non-Doppler radars were able to detect cloud boundaries, precipitation, and the melting layer. Despite its success in cloud detection, the AN/TPQ-11 suffered from hardware failures and eventually was retired from service. There was little further development or application of these shorter-wavelength radars for two decades due to the lack of hardware components at high frequencies and the early emphasis in radar meteorology given to precipitation studies, weather forecasting, and severe weather warning using centimeter-wavelength radars. This was the state of affairs until hardware and data-processing advances in the 1980s (Mead et al. 1994).

Table 1. Historical progression of millimeter-wavelength radar development in the United States.

Year	Reference/affiliation	Radar characteristics
Mid-1960s	Petrocchi and Paulsen (1966), Paulsen et al. (1970); U.S. Air Force	35-GHz, non-Doppler, vertically pointing
1983	Hobbs et al. (1985); University of Washington	35-GHz, Doppler, vertically pointing
1983	Pasqualucci et al. (1983); NOAA/Wave Propagation Laboratory	35-GHz Doppler, dual-polarization, scanning
1987	Lhermitte (1987); University of Miami	94-GHz, Doppler, vertically pointing
1993	Pazmany et al. (1994), Vali et al. (1995); University of Wyoming	94-GHz, Doppler, polarimetric, airborne
1996	Sekelsky and McIntosh (1996); University of Massachusetts	35/94-GHz, Doppler, polarimetric, scanning
1998	Moran et al. (1998); NOAA/Environmental Technology Laboratory	35-GHz, Doppler, pulse compression, unattended
2003	Racette et al. (2003), Li et al. (2004); NASA Goddard Space Flight Center	94-GHz, Doppler polarimetric, high altitude
2004	Stephens et al. (2002); Colorado State University/NASA Jet Propolsion Laboratory	94-GHz, non-Doppler, spaceborne; CloudSat
2005	Majurec et al. (2005); University of Massachusetts	14, 35, and 94 GHz, Doppler, polarimetric, scanning
2005	Farquharson et al. (2005); NCAR	35-GHz, coscanning with S-Pol

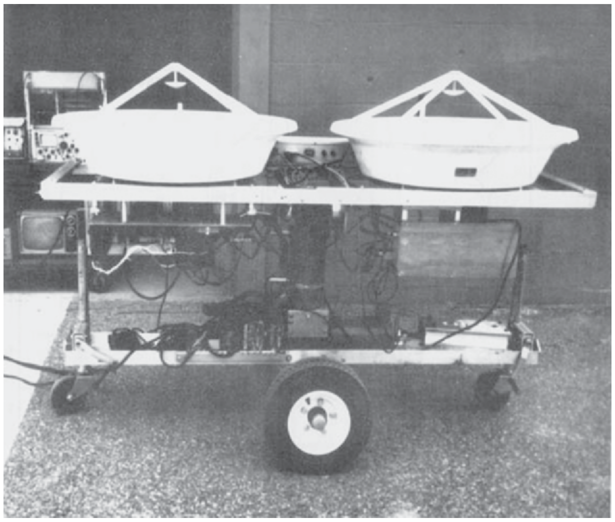

Fig. 3. Photograph of the prototype bistatic 94-GHz Doppler radar developed at the University of Miami by Roger Lhermitte (photo courtesy of Roger Lhermitte).

In the early 1980s Hobbs et al. (1985) modernized one of the surplus AN/TPQ-11 systems using solid-state electronics, the addition of Doppler capability, and improved data-display capabilities. Around the same time the National Oceanographic and Atmospheric Administration (NOAA) added dual-polarization and scanning capability to another surplus AN/TPQ-11 system (Pasqualucci et al. 1983; Martner et al. 2002). The development of these two systems marked a shift in cloud radar research from the military to university- and laboratory-based research groups. Another advance in cloud radars during the 1980s was the development of the first 94-GHz Doppler radar (Fig. 3) by Lhermitte (1987). To date the 94-GHz radar remains the highest-frequency (shortest wavelength) radar used for atmospheric cloud research.

Collaboration between the University of Wyoming and the Microwave Remote Sensing Laboratory (MIRSL) of the University of Massachusetts resulted in the design and development of the first airborne dual-Doppler and polarimetric 94-GHz radar (Pazmany et al. 1994; Vali et al. 1995). Designed to fly with the University of Wyoming King Air aircraft, this 94-GHz radar extended the observing capabilities of the aircraft beyond the in situ microphysics and turbulence probes and provided a cross section of the sampled clouds. In addition to the airborne radar system, MIRSL developed a mobile, truck-mounted cloud-profiling radar system (CPRS) with dual-frequency (35-/94-GHz), dual-polarization, and scanning capabilities (Sekelsky and McIntosh 1996). Another important development was the 94-GHz airborne radar that flew on the National Aeronautics and Space Administration's (NASA's) DC8 (Sadowy et al. 1997). That radar was an important test bed for the development of the spaceborne CloudSat radar.

In the mid-1990s the U.S. Department of Energy (DOE) Atmospheric Radiation Measurement (ARM) program deployed vertically pointing 35-GHz Doppler radars as the centerpiece of their observing instruments for the continuous monitoring and study of all radiatively important clouds at several climatologically distinct locations (Ackerman and Stokes 2003). These millimeter-wavelength cloud radars (MMCRs) were designed, developed, and placed at the ARM sites by NOAA (Moran et al. 1998). These radars use various operational modes, long signal dwells, and pulse compression to provide accurate radar reflectivity measurements over a dynamic range of approximately seven orders of magnitude (i.e., from −50 to +29 dBZe; see sidebar for more information on dBZ) throughout the troposphere. The ARM cloud radars have exhibited high reliability with data collection at the ARM sites occurring over 90% of the time. Deployment of the ARM program millimeter-wavelength cloud radars marked the beginning of a new era in application of millimeter-wavelength cloud radars to problems in atmospheric cloud research (Fig. 1). For the first time they had emerged as a critical component both for the long-term monitoring of clouds and their effects on Earth's radiation budget and for the improvement of cloud parameterizations in cloud-resolving and global climate models.

The ARM program currently has the largest collection of continuously operating millimeter-wavelength radars for atmospheric research in Oklahoma, Alaska, Australia, and Manus and Nauru Islands in the tropical western Pacific. In addition to its MMCRs the ARM program recently acquired two highly sensitive ground-based polarimetric 94-GHz Doppler radars for use with the ARM Mobile Facility (AMF; Miller and Slingo 2007) and the ARM continental Southern Great Plains (GPS) site in Oklahoma (Mead and Widener 2005). These newly built 94-GHz radars embrace the latest technological trends in millimeter-wavelength radar technology with digital receivers, low-noise front ends to the receivers, and sophisticated internal calibration procedures. Millimeter-wavelength cloud radars similar to those used by ARM are now in operation at Geestacht, Germany, Chilbolton, United Kingdom, Cabauw, the Netherlands, and Palaiseau, France

(Illingworth et al. 2004). In addition, the Canadians operate an MMCR (built by NOAA) at their Polar Environment Atmospheric Research Laboratory (PEARL) site at Eureka, Northwest Territories, Canada.

The use of a 94-GHz radar on NASA's high-altitude Earth Resources-2 (ER-2) platform (Racette et al. 2003; Li et al. 2004), the development of the University of Massachusetts Advance Multi-Frequency Radar (Majurec et al. 2005), the use of a 35-GHz radar as a second frequency to the National Center for Atmospheric Research (NCAR) S-band dual-polarization Doppler (S-Pol) radar (Farquharson et al. 2005), and the launch of the first spaceborne 94-GHz radar in April 2006 as part of the CloudSat Mission (Stephens et al. 2002) culminate the frantic development and use of millimeter-wavelength radars in atmospheric cloud research over the past 20–30 yr. Deployment of millimeter-wavelength radars in space is the beginning of a second era of application of these radars to atmospheric cloud research, allowing for global monitoring of clouds and precipitation.

WHY USE MILLIMETER-WAVELENGTH DOPPLER RADARS IN ATMOSPHERIC RESEARCH? A large fraction of the clouds present at any time in the Earth's atmosphere is composed of high concentrations of small hydrometeors, such as cloud droplets and ice crystals with diameters from a few to tens of micrometers. For these particles with diameters that are small compared with the radar wavelength, the equivalent reflectivity factor Z_e is written simply as the reflectivity factor Z (mm^6 m^{-3}), where $Z = \int n(D)\, D^6\, dD$ and $n(D)$ is the particle size distribution (m^{-3} m^{-1}). That is, Z is proportional to the sixth power of hydrometeor diameter D and is a number that allows scientists to compare data from radars that use different wavelengths. These clouds, composed of hydrometeors with diameters from a few to tens of micrometers, have very small radar reflectivity values. For example, a few tenths of a gram of liquid water per cubic meter distributed across a large number of small cloud droplets can have a radar reflectivity from −60 to −40 dBZ, and hence present a detection challenge for centimeter-wavelength (e.g., 10 cm) Doppler radars with minimum detectable

WHAT IS MEASURED BY A DOPPLER RADAR?

When an electromagnetic pulse is emitted by a radar transmitter, an accurate timer is started that measures the elapsed time from initiation of the pulse to the time of return of power scattered back to the radar from atmospheric particles. The elapsed time of a power return and the speed of light are subsequently used to infer the distance from the radar to the scattering particles; hence, radar data are range-resolved. Atmospheric particles are distributed in space and, over distances of a few to tens of millimeters, their positions are random. The amplitude and phase of the scattered electromagnetic waves from all of the particles within the radar pulse are random due to constructive and destructive interference.

Atmospheric particles are not fixed in space and they do not have fixed spatial locations with respect to each other. From pulse to pulse the amplitude A of the (superposed) electromagnetic wave scattered back to the radar fluctuates, leading to a distribution of amplitudes A that is described by the Rayleigh probability distribution (Marshall and Hitchfeld 1953). This leads to an exponential-like probability distribution for the backscattered power A^2 from the particles, with the average over all of the powers in the distribution proportional to the total particle backscattering cross section per unit volume. Each of the data points in a radar range versus time display of return power is a measure of the average power scattered by atmospheric particles to the radar. This power is converted to an estimate of the radar reflectivity η (mm^2 m^{-3}), or the total backscattering cross section σ_b (mm^2) of the atmospheric particles per cubic meter. The radar reflectivity η and total backscattering cross section σ_b depend on the radar wavelength. In the radar meteorological literature the radar equivalent reflectivity factor Z_e is generally used in place of η, where Z_e is defined by $Z_e = (\lambda^4 \eta)/(\pi^5 K^2)$ (mm^6 m^{-3}). In this relationship λ is the wavelength of the radiation in the radar pulse and K is a physical constant related to the properties of water. The equivalent radar reflectivity factor Z_e is independent of radar wavelength if the hydrometeor's maximum diameter D is much smaller than the radar wavelength and the scattering is described by the Rayleigh approximation. Because Z_e can span many orders of magnitude, it is generally presented in imagery on the logarithmic scale $10 \log_{10} Z_e$ and labeled with units of dBZ_e.

Doppler radars are those radars equipped with the necessary hardware to monitor the phase change of the backscattered signal from pulse to pulse. The phase shift from pulse to pulse contains information on the motions of the atmospheric particles relative to the radar. Transforming the time series of backscattered powers using a Fourier transform, we end up with a series (Doppler spectrum) of particle backscattering cross sections where each cross section is associated with different velocities (frequency shifts) toward or away from the radar. The total backscattered power to the radar (zeroth moment), the mean Doppler velocity (first moment), and the Doppler spectrum width (second moment), or standard deviation of the Doppler velocities, are often used in radar data analysis.

signals around –20 dBZ. The detection of such clouds with centimeter-wavelength radars requires the use of high-power transmitters and large antennas to achieve the needed radar sensitivity; radars of this type are not available for atmospheric cloud research.

To add perspective to this statement, consider one of the long-standing problems in atmospheric research: understanding the physical mechanisms responsible for the onset of precipitation in shallow warm clouds together with the associated broadening of drop size distributions (Beard and Ochs 1993). According to Knight and Miller (1993), Bragg scattering limits the usefulness of single-wavelength radars for studies of hydrometeor growth to radar reflectivity factors above about 10 dBZ for 10-cm-wavelength radars and 0 dBZ for 5-cm-wavelength radars. Such reflectivity values correspond to shallow clouds that have already developed a rain shaft and have already passed the stage of size spectral broadening. Millimeter-wavelength radars observe shallow cumuli and other cloud types well before they develop large hydrometeors. More generally, the advantages of using millimeter-wavelength radars in atmospheric research are several fold.

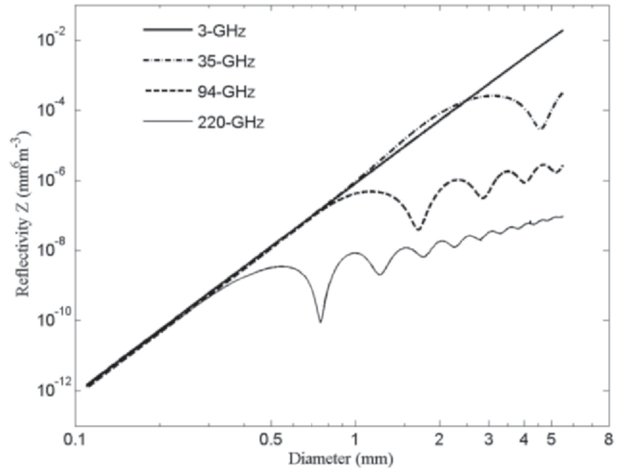

Fig. 4. The radar reflectivity as a function of spherical particle diameter for four different radar frequencies: 3 (solid line), 35 (dashed–dot line), 94 (dashed line), and 220 GHz (thin solid line). The particle concentration is 1 m^{-3}. Rayleigh backscattering is valid for all raindrop sizes at 3 GHz. At higher radar frequencies, deviation from the 3-GHz solid line indicates the maximum raindrop size for which the Rayleigh approximation is valid. As the raindrop size increases, there is a decrease in the radar reflectivities and mean Doppler velocities at higher frequencies.

Supplement the dynamic range of centimeter-wavelength radars. In the Rayleigh scattering regime (scattering by particles that are small compared with the wavelength) the radar reflectivity factor Z is independent of radar wavelength and the radar backscattering cross section σ_b (mm^2) is proportional to λ^{-4}. As a result, the use of ever-shorter radar wavelengths can significantly increase the backscattering cross section of small hydrometeors and make possible their detection without the use of high-power transmitters and large antennas. For example, the backscattering cross section of small scatterers is greater by 42 dB (a factor of $10^{4.2}$) at 35 GHz and 60 dB (a factor of 10^6) at 94 GHz than for a 3-GHz weather radar, for example, the Weather Surveillance Radar-1988 Doppler (WSR-88D; Fig. 4). That is, a cloud droplet scatters 1,000,000 times more of the incident irradiance for radars operating at 0.3- than at 10-cm wavelengths.

The backscattering cross-sectional dependence on radar wavelength imposes no constraints on the wavelength, implying that the use of the shortest possible radar wavelength is optimal in atmospheric research. This is not quite the reality. Absorption by atmospheric gases and hydrometeors, as well as technological limitations, place constraints on the optimal wavelengths for radar (Fig. 2). The absorption lines of H_2O (at 23 and 183 GHz) and O_2 (at 60 and 118 GHz), as well as the entire rotational band of H_2O at wavelengths shorter than 300 GHz (i.e., 1 mm), restrict the available radar frequencies to those below 300 GHz. At 35 (λ = 8.6 mm) and 94 (λ = 3.2 mm) GHz, attenuation from gases, especially in the Tropics, is significant. In the tropical boundary layer the specific humidity can reach values as high as 20–25 g kg^{-1} and the signal attenuation can reach 0.35 dB km^{-1} ($10^{-0.035}$, or 92%, km^{-1}) at 35 GHz and 2.0 dB km^{-1} ($10^{-0.2}$, or 63%, km^{-1}) at 94 GHz. Signal attenuation induced by hydrometeors, especially in the liquid phase, at these high radar frequencies is also significant. For example, 1 g m^{-3} of liquid distributed across a distribution of cloud droplets can cause two-way attenuation of 0.8 dB km^{-1} at 35 GHz and 4.0 dB km^{-1} at 94 GHz. The use of even higher radar frequencies, 140 and 220 GHz, has certain advantages, but the strong signal attenuation from gases and hydrometeors at these frequencies limits the application of these radars to ranges of a few kilometers or less. As a result, millimeter-wavelength radars (especially at 94 GHz) are heavily attenuated by precipitation and thus cannot provide useful information about rain when they scan. On the contrary, the attenuation of millimeter-wavelength radars in ice is very small (0.03 dB km^{-1} at 94 GHz for 1 g m^{-3} of ice), and thus makes them suitable for the study of mid- and upper-tropospheric clouds (e.g., Reinking et al. 2001; Stephens et al. 2002; Reehorst and Koengin 2004).

Dual-wavelength measurements and non-Rayleigh scattering. The Rayleigh scattering approximation ($\sigma_b \sim D^6/\lambda^4$) is valid as long as the size parameter $\pi D/\lambda$ of the particles is much smaller than unity. When millimeter-wavelength radars are used to study large hydrometeors, such as raindrops and large snowflakes, the size parameter approaches unity or higher. For such large particles the Rayleigh approximation is not valid and full theoretical solutions to scattering by particles of different shapes are necessary. Mie (1908) theory scattering solutions are used to describe the scattering and absorption of radar waves by spherical particles of any size. Hydrometeor shapes often deviate from spheres and more complex scattering solutions that account for the deviations are necessary (e.g., T matrix; see Mishchenko 2000; Mishchenko et al. 2002; Yang et al. 2003). For simplicity we limit our discussion to spherical particles and results from Mie theory. We use the phrase "non-Rayleigh regime" to denote scattering from liquid water spheres with diameters comparable to or greater than the radar wavelength (Stephens 1994).

In the non-Rayleigh scattering regime the backscattering cross sections of raindrops do not monotonically increase with the sixth power of the particle diameter; rather, they exhibit a quasi-periodic form with exponential damping of the oscillation. Figure 4 shows sphere backscattering cross sections as a function of sphere diameter for various frequencies. At 3 GHz, scattering by spherical raindrops is described by the Rayleigh approximation with a monotonic increase of the backscattering cross section with size. As the radar frequency increases, the non-Rayleigh scattering regime is eventually reached with several noticeable features.

First, in the Rayleigh regime the scattering cross section is always small compared with the absorption cross section. In the non-Rayleigh regime scattering is of equal importance to absorption. Their combined effect (extinction) is large. For example, the extinction coefficient of raindrops at 94 GHz is 1000 times that at 3 GHz. Severe extinction of the radar beam limits the use of short-wavelength radars for probing precipitation systems.

Second, it is apparent in Fig. 4 that when the non-Rayleigh regime is entered, there is a particle backscattering "deficit" compared with lower radar frequencies. This results in lower predicted, and observed, radar reflectivities in rain from millimeter-wavelength radars. For example, 100 mm h^{-1} surface rainfall produced by an exponential Marshall and Palmer (1948) raindrop size distribution has a radar reflectivity above 50 dB*Z* at 3 GHz, but 47 dB*Z*e at 35 GHz, and below 30 dB*Z*e at 94 GHz. Scattering in the non-Rayleigh regime suppresses the dynamic range of observed radar reflectivity values in rain with decreasing radar wavelength. Entering the non-Rayleigh scattering regime also affects the observed mean Doppler velocity of raindrop size distributions from vertically pointing (vertically profiling) radars. The suppression of large particle contributions to the Doppler spectrum with decreasing radar wavelength increases the relative contribution of small raindrops during rain and shifts the observed mean Doppler velocity to lower magnitudes (Fig. 5).

And third, the non-Rayleigh scattering regime for vertically profiling millimeter-wavelength radars produces quite a different view of precipitation than the one described in radar meteorology textbooks and that is used to classify precipitation in convective or stratiform rain. For example, convective precipitation is often described as a vertically oriented high-reflectivity (>35 dB*Z*) core when observed from ground-based, airborne, or spaceborne radar. However, millimeter-wavelength radars have suppressed radar reflectivities in rain and values as large as 35 dB*Z* are rarely, if ever, observed.

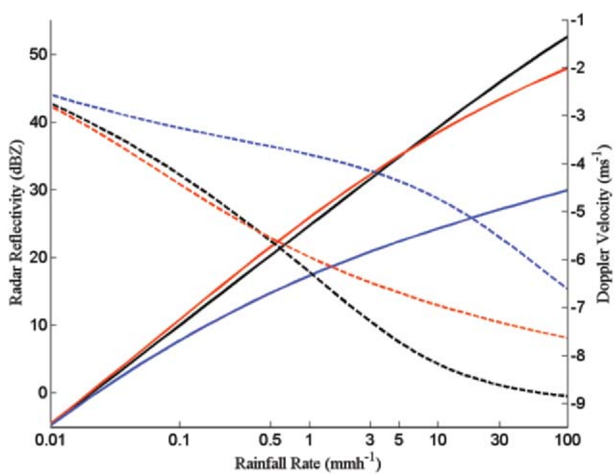

Fig. 5. Reflectivity (dB*Z*, solid lines) and mean Doppler velocity <V>$_{Dop}$ (m s^{-1}, dashed lines, radar is vertically pointing) as a function of the rainfall rate *R* (mm h^{-1}) for an exponential raindrop size distribution $N(D) = N_o e^{-\Lambda D}$ (Marshall and Palmer 1948) and for three radar frequencies at 3 (black line), 35 (red line), and 94 (blue line) GHz. The differences in the backscattering cross section as a function of the diameter among the different radar frequencies result in differences in the Doppler moments (reflectivity, mean Doppler velocity, and Doppler spectrum width) calculated at each radar frequency.

Strong signal attenuation limits the penetration of millimeter-wavelength radar signals to a couple of kilometers into the precipitation layer at high rainfall rates (Kollias et al. 2003), and thus no vertically oriented high-reflectivity structure is observed. Even more striking is the diminishing (at 35 GHz) or complete lack (at 94 GHz) of the radar brightband signature (e.g., Sassen et al. 2005; Kollias and Albrecht 2005), one of the most distinct radar textbook features that is often used to identify stratiform precipitation. Empirical and theoretical relationships between radar reflectivity and rainfall (*Z*–*R*) developed for low-frequency radars are not applicable at millimeter wavelengths. The sensitivity of millimeter-wavelength radars allows them to detect drizzle and leads to the development of their own *Z*–*R* relationships at small rainfall rates (e.g., Wang and Geerts 2003; Comstock et al. 2004).

The complications that arise from the scattering of particles with diameters comparable with or larger than the radar wavelength, that is, drizzle and raindrops, and to some extent large snowflakes, could discourage the use of millimeter-wavelength radars for precipitation research. Attenuation and non-Rayleigh scattering do complicate the interpretation of the observed radar reflectivity, especially in scanning modes, but signal attenuation and non-Rayleigh scattering at millimeter wavelengths depend on the details of the hydrometeor size distribution and can be used to constrain retrievals of cloud and precipitation microphysics, especially when dual-frequency radar observations are used (e.g., Hogan et al. 2005; Martner et al. 1993; Matrosov 1998; Sekelsky and McIntosh 1996). Measurements from a 94-GHz profiling Doppler radar combined with those from lower-frequency radars are useful for analyzing the microphysics and kinematics associated with both convective and stratiform rain (e.g., Kollias et al. 2003).

Less susceptible than centimeter-wavelength radars to Bragg scattering. Another factor limiting the use of centimeter-wavelength radars for cloud research in the lowest 2–3 km of the troposphere is Bragg scattering (Fig. 6); these are backscattered returns caused by variations in water vapor (or refractive index) associated with turbulence (e.g., Knight and Miller 1998; Doviak and Zrnić 1993). Miller et al. (1998) verified that the National Weather Service WSR-88D operating at a 10-cm wavelength has the sensitivity to detect nonprecipitating clouds, but Bragg scattering from refractive index inhomogeneities can be of the same magnitude as cloud returns under many conditions, whereupon interpretation of WSR-88D reflectivities can be either complicated or impossible.

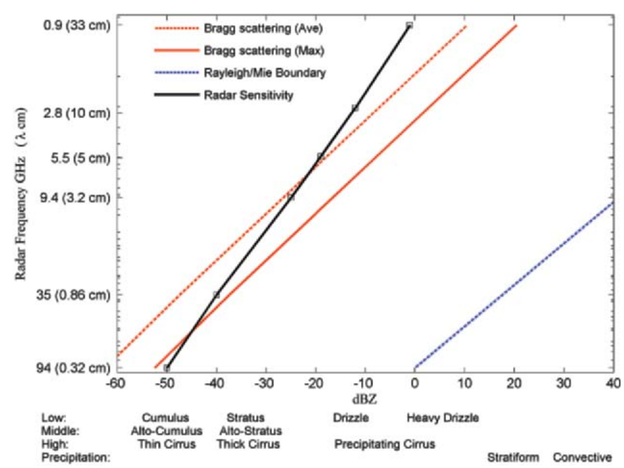

Fig. 6. At millimeter wavelengths observed radar reflectivities originate almost exclusively from hydrometeors. At longer wavelengths Bragg scattering can mask the backscattered returns from clouds, precluding reliable use of even the most sensitive centimeter-wavelength radars for cloud studies. The equivalent radar reflectivity resulting from Bragg scattering as a function of radar frequency for average and extreme values of the refractive index structure constant C^2_n, which depends on spatial fluctuations in the moisture field (Gossard and Strauch 1983), is illustrated here. The blue line shows the transition boundary from the Rayleigh approximation to non-Rayleigh scattering as a function of the radar frequency (wavelength) and equivalent radar reflectivity. The red lines show the point where the backscattered radar signal from clouds equals the expected backscattered radar signal from Bragg for average (dashed red line) and extreme (solid red line) refractive index variations. For a given radar frequency, observed echoes to the right of the Bragg lines have contributions mostly from hydrometeors, while observed echoes to the left of the Bragg lines have contributions mostly from Bragg scattering. The black line shows examples of operational radar sensitivity of well-known radar systems: the NOAA wind profiler network at 0.915 GHz (range 5 km), the WSR-88D at 2.7 GHz (range 20 km), the Bureau of Meteorology C-band dual-polarization Doppler radar (C-Pol; 5.5 GHz) scanning radar (range 20 km), the NOAA Physical Science Division 9.4-GHz radar (2-km range), the 35-GHz ARM MMCR (2-km range), and the ARM 94-GHz Mobile Facility radar (5-km range). The radar sensitivity curve is specific to the system chosen and it is not representative of what new technologies can yield at these frequencies.

Less susceptible to ground clutter. In addition to Rayleigh gain there are several other factors that suggest the benefits of millimeter-wavelength radars for cloud studies. The most important consideration for short-range (a few kilometers) detection of weak atmospheric targets is not only the sensitivity of the radar, but also ground echoes (clutter) that leak into the returns through the antenna sidelobes. Ground clutter occurs when fixed objects, such as buildings, trees, or terrain, are intercepted by the radar beam and produce nonmeteorological echoes. This is especially a problem for high-power long-wavelength radars.

The variation of ground clutter cross sections σ^0 per unit area as a function of radar wavelength is not well known and depends on the targets. Long (1983) shows that, on average, σ^0 is proportional to λ^{-1}. As we have seen, cloud-drop echo intensities increase proportionally to λ^{-4}, for a dramatic increase of 60 dB from 10- to 0.32-cm wavelengths. Even with a 10-dB increase in σ^0 with the shorter wavelengths, the ground-clutter-to-cloud-return contrast will improve by at least 50 dB from 10- to 0.3-cm wavelengths (e.g., Kropfli and Kelly 1996). Our experience is that when surrounded by buildings and trees a 94-GHz cloud radar does not show any measurable ground clutter signal at short ranges.

Millimeter-wave radars operated in a vertically pointing mode, or off vertical if three-dimensional scanning is required, are an attractive solution for the observation of low-altitude, low-reflectivity clouds, such as fair-weather cumuli. In addition, the far-field range of approximately $2D_a^2/\lambda$, where D_a is the antenna diameter and λ is the radar wavelength, is much larger for centimeter-wavelength radar antennas with the same beamwidths as typical millimeter-wavelength radars; hence, vertically pointing centimeter-wavelength radars are unable to produce useful data as close to the surface as their millimeter-wavelength counterparts.

Deployable on mobile systems. Operated from mobile (e.g., research aircraft and ship) platforms, millimeter-wavelength radars can sample larger volumes of clouds in a variety of conditions. These platforms are used in intensive observing periods and produce measurements relevant to cloud-scale physical processes. Examples of such cloud radar systems are the University of Wyoming King Air 94-GHz cloud radar (Vali et al. 1995) and the sea-going NOAA Physical Science Division (PSD) 35-GHz MMCR (e.g., Kollias et al. 2004). The airborne cloud radar provides an instantaneous depiction of reflectivity and velocity fields at high spatial resolution that are coincident with observations of detailed microphysics and air motions provided by the other probes carried on the aircraft platform (e.g., French et al. 2000; Vali et al. 1998; Leon and Vali 1998).

Applications of millimeter-wavelength cloud radars in atmospheric research. Millimeter-wavelength radars have adequate sensitivity to detect nonprecipitating clouds, such as fair-weather cumuli in the boundary layer and thin cirrus aloft, excellent Doppler velocity resolution to observe the small fall velocities of small ice crystals and cloud droplets, and are unaffected by Bragg scattering and ground clutter. These advantages of millimeter-wavelength radars make them suitable for the detection of weak nonprecipitating clouds that are often not well characterized by radars operating at longer wavelengths, such as the U.S. WSR-88D Next-Generation Weather Radar (NEXRAD) network. This leads to a plethora of applications exclusively in the domain of millimeter-wavelength radars.

Cloud layer statistics. Currently, there are five stationary sites and one mobile site operated by the ARM program that provide continuous measurements of clouds and radiation (Stokes and Schwartz 1994; Ackerman and Stokes 2003). CloudNet, a research project supported by the European Commission to evaluate the representation of clouds in major European weather forecast models, also operates a network of three cloud remote sensing (CRS) stations with millimeter-wavelength radars as part of their basic instrumentation (e.g., Illingworth et al. 2004). These ground-based cloud radars resolve the vertical distribution of cloud layers and are able to produce statistics of cloud fractions with altitude, cloud boundary heights, and radar reflectivities (Fig. 7a) for various types of clouds (e.g., Dong et al. 2005; Hogan et al. 2001; Lazarus et al. 2000). If a radar system is run continuously over a number of years at a particular location, it eventually samples the full range of dynamical and microphysical regimes typical of that location's climate (Fig. 7b). If additional datasets are used to put the cloud-layering information into the context of large-scale, or mesoscale, dynamical regimes, such information can be used to study interactions among dynamical and microphysical processes and to evaluate the ability of models to simulate those interactions.

Turbulence, microphysics, and process studies in clouds and precipitation. When pointing vertically,

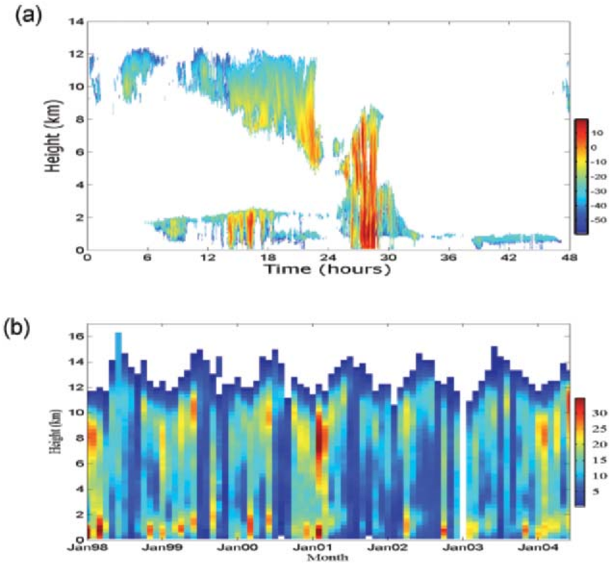

Fig. 7. (a) Example of 48 h of profiles of radar reflectivity (dBZe) from the MMCR located at the ARM Southern Great Plain site showing the passage of a frontal system. Note the ability of the millimeter-wavelength radar to observe high-altitude cirrus clouds, precipitation, and boundary layer clouds. (b) Monthly averaged cloud fraction (%) at the ARM SGP site derived from a long record of continuous, high-resolution radar observations from the ARM MMCR.

radars observe the vertical velocity component of hydrometeors, which is the sum of particle terminal fall velocity and the vertical air motion. Applying fast Fourier transforms to time series of received radar signals, the distribution (Doppler spectrum) of backscattering cross section versus vertical velocity is created, and, as we mentioned earlier, the moments of the Doppler spectrum, that is, reflectivity, mean Doppler velocity, and Doppler spectrum width, are often used. Although these observables are obtainable by all radars, millimeter-wavelength radars detect both small and large particles, and have high temporal and spatial resolutions and high velocity resolution (Kollias et al. 2002). These attributes of millimeter-wavelength radars make them suitable for the study of turbulence, microphysics, and cloud-scale processes that act at small scales.

The terminal velocity of small particles (e.g., cloud droplets and ice crystals) is small and the observed vertical velocities of these small particles are mainly due to air motion and turbulence. Under these circumstances, any broadening of the Doppler spectrum that results from variations in particle size is overwhelmed by turbulence and wind-shear broadening. For clouds containing small particles, the mean Doppler velocity and Doppler spectrum width have strong contributions from turbulence (Kollias et al. 2001) and the observed Doppler information is used for the study of cloud updraft–downdraft structures, turbulence intensity, gravity waves, and entrainment (e.g., Damiani et al. 2006; Kollias and Albrecht 2000; O'Connor et al. 2005).

In addition to retrieval of cloud kinematics using millimeter-wavelength radars, techniques for retrieving cloud, ice crystal, and drizzle particle size distributions have been developed (e.g., Gossard 1988; Gossard 1994; Hogan et al. 2000; Frisch et al. 1995; Babb et al. 1999; Mace et al. 2002; Matrosov et al. 2002; O'Connor et al. 2005; Sekelsky et al. 1999). In certain circumstances millimeter-wavelength radar Doppler spectra can be used to estimate the microphysical composition of both phases of mixed-phase clouds (Shupe et al. 2004). Another area of millimeter-wavelength radar research is the identification of cloud particle types (e.g., cloud droplets, drizzle, ice crystal habits) using polarimetric measurements (e.g., Reinking et al. 2002). These techniques demonstrate that, when combined with microwave radiometer and lidar measurements, millimeter-wavelength radars are a powerful research tool for the study of cloud microphysics.

Radars operating at 94 GHz provide a novel approach, first proposed by Lhermitte (1988), for retrieving precipitation drop size distributions and vertical air motions simultaneously (Fig. 8). In the non-Rayleigh scattering regime the backscattering cross section as function of raindrop diameter oscillates at 94 GHz due to resonant electromagnetic multipole effects. Under precipitating conditions, these oscillations are apparent in the observed Doppler spectra (Fig. 8) and can be used as reference points for the retrieval of the vertical air motion and subsequently the precipitation drop size distribution (Kollias et al. 2002; Firda et al. 1999). Combined with centimeter-wavelength radars, 94-GHz radars can provide high spatial and temporal measurements in stratiform and convective rain (Kollias et al. 2003).

FUTURE OUTLOOK OF CLOUD RADAR APPLICATIONS. Trends in the number and applications of millimeter-wavelength radars in atmospheric cloud research suggest that we have entered a new phase of exciting developments similar to those observed in the 1980s. As is the case for most significant advancements in atmospheric observations, this recent surge in cloud radar applications is driven by new eminent scientific needs and emerging technological developments in the field of radar meteorology. One recent technological advance, the development of sophisticated pulse compression waveforms, will further boost sensitivity of cloud radars to –50 dB*Z* at several kilometers of range, allowing the use of low-peak powers and hence low-cost transmitters. Versatile, adaptive, and fast digital receivers with adequate dynamic range and near-100% data processing efficiency are already available, further improving the performance of cloud radars and resulting in the replacement of several analog radar components with inexpensive computer-based cards that offer greater flexibility and robust radar operation. The miniaturization and integration of radar components will further decrease the size, weight, and power requirements of millimeter-wavelength radars and ease their deployment on moving platforms. The main constraint on the widespread use and application of cloud radars by laboratories and academic institutions is their high cost related to design, fabrication, and maintenance.

In April 2006 the first spaceborne 94-GHz cloud radar was launched as part of the CloudSat mission (Stephens et al. 2002). CloudSat is an experiment that will use radar to study clouds and precipitation from space and will fly in orbital formation as part of the A-Train constellation of satellites (Fig. 9). As part of its future Global Precipitation Measurements (GPM) program (currently scheduled for launch in 2013), NASA will launch a dual-frequency (13.6/35 GHz) precipitation radar to provide detailed three-dimensional measurements of cloud structure, rainfall, and rain

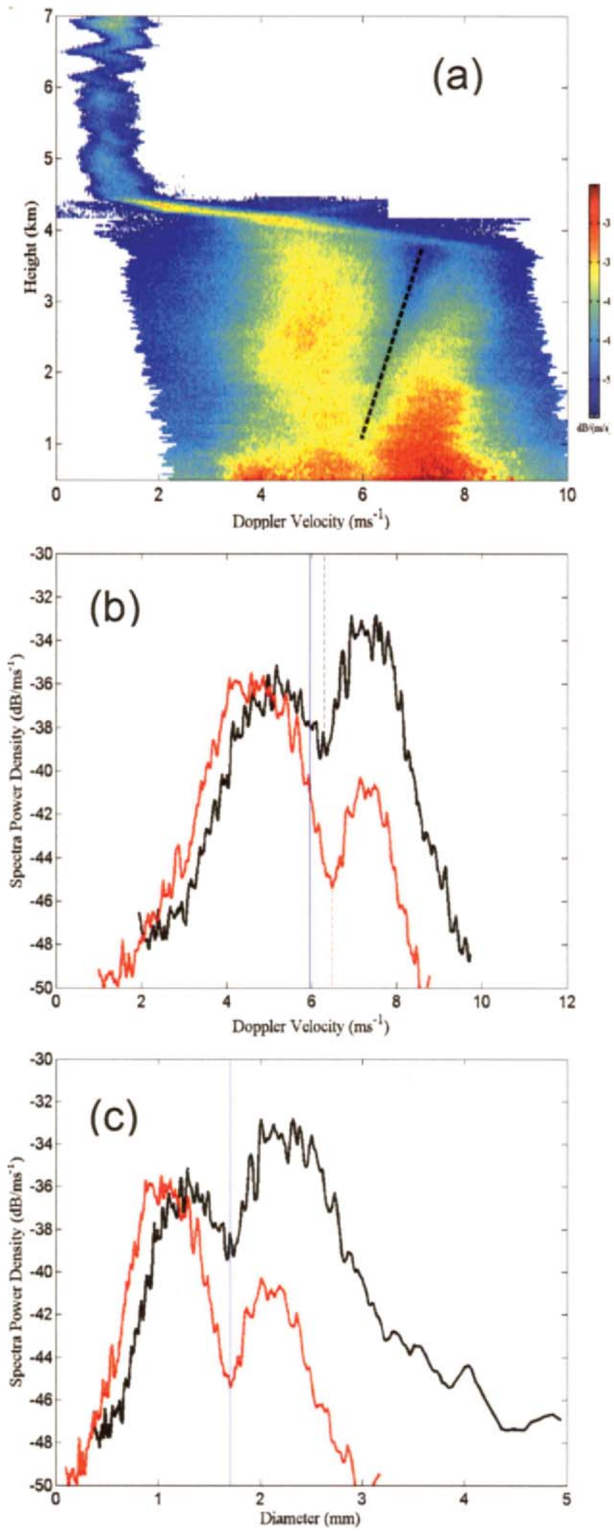

Fig. 8. (a) Example of Doppler spectrogram (stack of Doppler spectra with height) recorded by the University of Miami 94-GHz Doppler radar in stratiform rain. The black dotted line indicates the approximate location of the first Mie scattering minimum that occurs around raindrop diameters of 1.7 mm (5.95 m s^{-1} fall velocity at surface conditions). The slope of the line indicates a shifting of the Mie minimum location with altitude that can be used to verify the change of the raindrop fall velocity with altitude due to differences in air density. (b) Examples of Doppler spectra near the surface from two different periods. The blue line indicates the location of the Mie minimum if no vertical air motion is present. Thus, the observed shift can be used to retrieve the vertical air motion with very good accuracy. If the observed Doppler spectra are shifted to correspond to zero vertical air motion, we can infer the raindrop diameter from the observed Doppler velocities, as we illustrate in the next panel. (c) The bimodal and often trimodal shapes of Doppler spectra at 94-GHz in rain are a direct result of the oscillatory backscattering cross section of raindrops at 94-GHz. Differences in the shapes of Doppler spectra are also due to differences in raindrop size distributions—the other factor that contributes to the shapes of Doppler spectra. In this example, the red Doppler spectrum contains more small raindrops and the black Doppler spectrum higher concentrations of large raindrops.

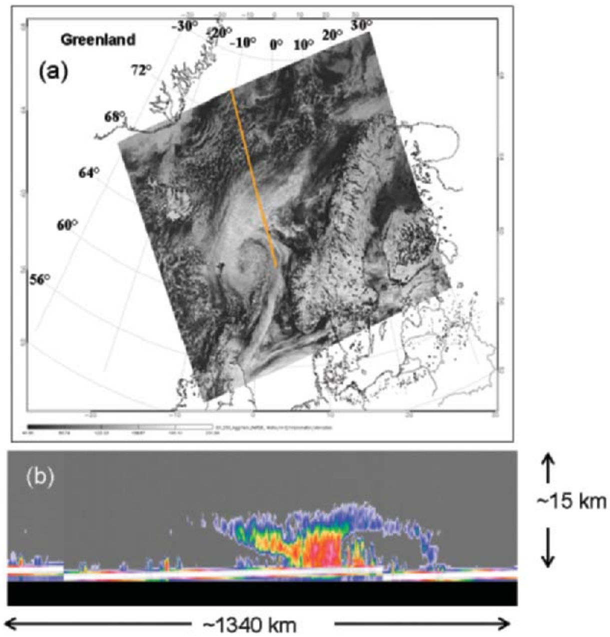

Fig. 9. (a) The cloud structures and a sense of the circulation are revealed in a visible image from the MODIS on the *Aqua* spacecraft; the image was collected minutes after the CloudSat view of the same storm. (b) The first light image from the CloudSat radar collected for approximately 30 s after initial transmission on 20 May 2006. The radar provides a cross-sectional view of the cloud and precipitation structures associated with a cyclonic disturbance that developed over the North Sea southeast of Greenland. The radar image provides a unique view of the warm-front sector.

rates. Recently, the European Space Agency (ESA), as part of its Earth Explorer Core mission, selected the Earth, Clouds, Aerosols, and Radiation Explorer (EarthCARE) mission with a spaceborne 94-GHz radar, which is intended for launch in 2012. The EarthCARE mission is a joint European–Japanese venture and aims to better understand the interactions between cloud, radiative, and aerosol processes that play a role in climate regulation. All of these spaceborne cloud radar missions will enhance our ability to monitor and study cloud and precipitation processes on a global scale.

The development of several new airborne cloud radar systems is underway. The Canadian National Research Council Institute for Aerospace Research (NRC Aerospace) is currently testing a state-of-the-art dual-frequency (9.4/94 GHz) airborne radar system onboard its Convair-580 research aircraft for atmospheric and flight safety research. The NRC airborne radar system will provide both a high resolution and high sensitivity for the detection of weakly scattering clouds. The system will have a fully polarimetric and Doppler measurement capability at both frequencies, pulse compression at 94 GHz, and digital receiver technology. NCAR proposed the installation of a 94-GHz cloud radar in its recently acquired High-Performance Instrumented Airborne Platform for Environmental Research (HIAPER). The U.S. Department of Energy (DOE) aerial vehicle program (AVP) is also planning the design and deployment of cloud radars for high-altitude platforms. Finally, the NOAA Physical Science Division is developing a shipborne 94-GHz cloud radar with stabilization for the removal of ship pitches and rolls for the study of marine stratus and trade wind cumulus.

Another continuously expanding application of cloud radars is their use in the context of large research programs, such as the U.S. DOE ARM and European CloudNet programs. The primary role of the ARM program is to help resolve scientific uncertainties related to global climate change, with a specific focus on the crucial role of clouds and their influence on radiative feedback processes in the atmosphere. The ARM cloud radars (MMCRs) provide continuous profiling observations of clouds and, combined with radiation measurements, are used to improve the treatment of cloud and radiation physics in numerical models, including global climate models. The European CloudNet program, with several sites in western Europe, also aims to improve the representation of clouds in numerical models. Countries, such as Japan and Canada, are also participating in the development and application of cloud radars as evidenced by their participation in programs with airborne and spaceborne cloud radars.

At present, the ARM MMCRs operate in a vertically pointing mode, providing a detailed view of the clouds that pass over the radar sites by continuously recording all Doppler spectra generated at each range. The need to address three-dimensional radiative transfer issues requires knowledge of three-dimensional cloud and precipitation structures. Consequently, the ARM program is organizing an effort to volume sample cloudy atmospheres with scanning cloud radar systems. It is possible that in the near future we will see the deployment of arrays of scanning cloud radars that map three-dimensional structures of clouds over small (e.g., 20 km × 20 km) domains at the ARM site in Oklahoma. Volume scanning with cloud radars, or with radars that have adequate sensitivity to detect weak clouds at long ranges, will have to be limited to ranges of approximately 20–30 km, which are much smaller than the traditional 150–200-km ranges of weather radar. This limitation on the cloud radars is imposed by differences in radar signal attenuation that result from water vapor and hydrometeors and different accuracy and resolution requirements for the measurements.

The detection envelope of weather radars is often limited to precipitating clouds. For radiative transfer and cloud-modeling applications all cloud and hydrometeor types are important. Many aspects of the three-dimensional mapping of clouds and precipitation represent a challenge. Technologically, supersensitive radars, for example, −40 dB*Z* at 20-km range, need to be designed. New, innovative sampling strategies are required to sample adequately the three-dimensional structure of clouds with morphological and life cycle characteristics that are much different from precipitating systems. Polarimetric, Doppler, and multiwavelength radar techniques are required to achieve the required accuracy in retrieving cloud boundaries and microphysics.

EPILOGUE. This paper provides an overview of past and present research activities involving the development of cloud radars and associated retrieval techniques. Major developments in millimeter-wavelength radars since the overview by Kropfli and Kelly (1996) a decade ago include the following:

a) Numerous cloud radars are now operated by several groups worldwide.
b) Long-term cloud monitoring with profiling cloud radars is well underway at several international locations, particularly by the ARM program. The ARM MMCR in Oklahoma recently (November 2006) completed 10 yr of continuous operations.
c) Spaceborne millimeter-wavelength radars are now a reality with the launch of CloudSat (and the future launch of the GPM satellite).
d) Cloud radars are currently deployed at mobile platforms (e.g., aircraft, ships).
e) Reliable, high-performance millimeter-wavelength radar components, and particularly 94-GHz transmitter/modulator systems, are now available.

The strengths of cloud radars are their cloud detection and resolution capabilities, their synergy with lidars and radiometers that result in sophisticated retrieval techniques, and their portability, which make them suitable for deployment on mobile platforms.

The need to understand cloud processes at ever-smaller spatial and temporal scales and, at the same time, to provide global cloud and precipitation coverage will, combined with technological advancements, further boost the use of millimeter-wavelength radars in atmospheric cloud research. The recent launch of the 94-GHz radar onboard CloudSat has initiated the application of millimeter-wavelength radars to retrieving cloud properties on a global scale. This feat, combined with the mature ground-based vertically pointing millimeter-wavelength radars, their future extension to scanning three-dimensional volumes of cloud, and the development of new millimeter-wavelength radars for airborne platforms, encouraged us to write this article at this time.

As cloud radar systems flourish, efficient analysis and application of their measurements to important problems will require a corresponding increase in the number of cloud radar meteorologists, or perhaps “non-Rayleigh” radar meteorologists. What proportion of the American Meteorological Society (AMS) radar conference participants know that a 94-GHz radar will not observe radar reflectivities higher than 30 dB*Z*e even under the most extreme rainfall conditions? Or that the radar signature at 94 GHz of hydrometeors in the melting layer is not an enhancement of the radar reflectivity? In the future, centimeter- and millimeter-wavelength radars will be integral parts of sophisticated observing facilities that will investigate both cloud and precipitation processes. This is the only way to evolve beyond the artificial state where we deal with clouds and precipitation as separate chains of events of the water cycle. In this direction, undergraduate- and graduate-level radar meteorology courses must give greater emphasis to high-frequency radar principles and data analysis techniques applicable to clouds (e.g., Doppler spectra-based retrievals).

REFERENCES

Ackerman, T. P., and G. Stokes, 2003: The Atmospheric Radiation Measurement program. *Phys. Today,* **56,** 38–45.

Atlas, D., Ed., 1990: *Radar in Meteorology.* Amer. Meteor. Soc., 806 pp.

Babb, D. M., J. Verlinde, and B. A. Albrecht, 1999: Retrieval of cloud microphysical parameters from 94-GHz radar Doppler power spectra. *J. Atmos. Oceanic Technol.,* **16,** 489–503.

Beard, K. V., and H. T. Ochs III, 1993: Warm-rain initiation: An overview of microphysical mechanisms. *J. Appl. Meteor.,* **32,** 608–625.

Brown, R. A., and J. M. Lewis, 2005: PATH TO NEXRAD: Doppler radar development at the National Severe Storms Laboratory. *Bull. Amer. Meteor. Soc.,* **86,** 1459–1470.

Clothiaux, E. E., M. A. Miller, B. A. Albrecht, T. P. Ackermann, J. Verlinde, D. M. Babb, R. M. Peters, and W. J. Syrett, 1995: An evaluation of a 94-GHz radar for remote sensing of cloud properties. *J. Atmos. Oceanic Technol.,* **12,** 201–229.

Comstock, K. K., R. Wood, S. E. Yuter, and C. S. Bretherton, 2004: Reflectivity and rain rate in and below drizzling stratocumulus. *Quart. J. Roy. Meteor. Soc.,* **130,** 2891–2919.

Damiani, R., G. Vali, and S. Haimov, 2006: The structure of thermals in cumulus from airborne dual-Doppler radar observations. *J. Atmos. Sci.,* **63,** 1432–1450.

Delamere, J. S., S. A. Clough, E. J. Mlawer, S.-A. Boukabara, K. Cady-Pereira, and M. Shepard, 2002: An update on radiative transfer model development at Atmospheric and Environmental Research, Inc. *Proc. 12th ARM Science Team Meeting,* St. Petersburgh, FL, ARM. [Available online at www.arm.gov/publications/proceedings/conf12/extended_abs/delamere-js.pdf.]

Dong, X., P. Minnis, and B. Xi, 2005: A climatology of midlatitude continental clouds from the ARM SGP central facility. Part I: Low-level cloud macrophysical, microphysical, and radiative properties. *J. Climate,* **18,** 1391–1410.

Doviak, R. J., and D. S. Zrnić, 1993: *Doppler Radar and Weather Observations.* 2d ed. Academic Press, 592 pp.

Farquharson, G., and Coauthors, 2005: NCAR S-Pol second frequency (Ka-band) radar. Preprints, *32d Conf. on Radar Meteorology,* Albuquerque, NM, Amer. Meteor. Soc., CD-ROM, P12R.6.

Firda, J. M., S. M. Sekelsky, and R. E. McIntosh, 1999: Application of dual-frequency millimeter wave Doppler spectra for the retrieval of drop size distributions and vertical air motion in rain. *J. Atmos. Oceanic Technol.,* **16,** 216–236.

French, J. F., G. Vali, and R. D. Kelly, 2000: Observations of microphysics pertaining the development of drizzle in warm, shallow cumulus clouds. *Quart. J. Roy. Meteor. Soc.,* **126,** 415–443.

Frisch, A. S., C. W. Fairall, and J. B. Snider, 1995: Measurement of stratus cloud and drizzle parameters in ASTEX with a Kα-band Doppler radar and microwave radiometer. *J. Atmos. Sci.,* **52,** 2788–2799.

Gossard, E. E., 1988: Measuring drop size distributions in cloud with a clear-air sensing Doppler radar. *J. Atmos. Oceanic Technol.,* **5,** 640–649.

——, 1994: Measurements of cloud droplet size spectra by Doppler radar. *J. Atmos. Oceanic Technol.,* **11,** 712–726.

——, and R. G. Strauch, 1983: *Radar Observation of Clear Air and Clouds.* Elsevier, 279 pp.

Hobbs, P. V., N. T. Funk, R. R. Weiss Sr., J. D. Locatelli, and K. R. Biswas, 1985: Evaluation of a 35 GHz radar for cloud physics research. *J. Atmos. Oceanic Technol.,* **2,** 35–48.

Hogan, R. J., A. J. Illingworth, and H. Sauvageot, 2000: Measuring crystal size in cirrus using 35- and 94-GHz radars. *J. Atmos. Oceanic Technol.,* **17,** 27–37.

——, C. Jakob, and A. J. Illingworth, 2001: Comparison of ECMWF winter-season cloud fraction with radar derived values. *J. Appl. Meteor.,* **40,** 513–525.

——, N. Gaussiat, and A. J. Illingworth, 2005: Stratocumulus liquid water content from dual-wavelength radar. *J. Atmos. Oceanic Technol.,* **22,** 1207–1218.

Illingworth, A. J., and Coauthors, 2007: Cloudnet: Continuous evaluation of cloud profiles in seven operational models using ground-based observations. *Bull. Amer. Meteor. Soc.,* **88,** 883–898.

Knight, C. A., and L. J. Miller, 1993: First radar echoes from cumulus clouds. *Bull. Amer. Meteor. Soc.,* **74,** 179–188.

——, and ——, 1998: Early radar echoes from small, warm cumulus: Bragg and hydrometeor scattering. *J. Atmos. Sci.,* **55,** 2974–2992.

Kollias, P,. and B. A. Albrecht, 2000: The turbulent structure in a continental stratocumulus cloud from millimeter wavelength radar observations. *J. Atmos. Sci.,* **57,** 2417–2434.

——, and ——, 2005: Why the melting layer reflectivity is not bright at 94-GHz. *Geophys. Res. Lett.,* **32,** L24818, doi:10.1029/2005GL024074.

——, ——, R. Lhermitte, and A. Savtchenko, 2001: Radar observations of updrafts, downdrafts, and turbulence in fair weather cumuli. *J. Atmos. Sci.,* **58,** 1750–1766.

——, ——, and F. D. Marks Jr., 2002: Why Mie? Accurate observations of vertical air velocities and raindrops using a cloud radar. *Bull. Amer. Meteor. Soc.,* **83,** 1471–1483.

——, ——, and ——, 2003: Cloud radar observations of vertical drafts and microphysics in convective rain. *J. Geophys. Res.,* **108,** 4053, doi:10.1029/2001JD002033.

——, C. W. Fairall, P. Zuidema, J. Tomlinson, and G. A. Wick, 2004: Observations of marine stratocumulus in SE Pacific during the PACS Cruise. *Geophys. Res. Lett.,* **31,** L22110, doi:10.1029/2004GL020751.

Kropfli, R. A., and R. D. Kelly, 1996: Meteorological research applications of MM-wave radar. *Meteor. Atmos. Phys.,* **59,** 105–121.

Lazarus, S. M., S. K. Krueger, and G. G. Mace, 2000: A cloud climatology of the Southern Great Plains ARM CART. *J. Climate,* **13,** 1762–1775.

Leon, D., and G. Vali, 1998: Retrieval of three-dimensional particle velocity from airborne Doppler radar data. *J. Atmos. Oceanic Technol.,* **15,** 860–870.

Lhermitte, R., 1987: A 94 GHz Doppler radar for clouds observations. *J. Atmos. Oceanic Technol.,* **4,** 36–48.

——, 1988: Observations of rain at vertical incidence with a 94 GHz Doppler radar: An insight of Mie scattering. *Geophys. Res. Lett.,* **15,** 1125–1128.

——, 1990: Attenuation and scattering of millimeter wavelength radiation by clouds and precipitation. *J. Atmos. Oceanic Technol.,* **7,** 464–479.

——, 2002: *Centimeter and Millimeter Wavelength Radars in Meteorology.* Lhermitte Publications, 550 pp.

Li, L., G. M. Heymsfield, P. E. Racette, L. Tian, and E. Zenker, 2004: A 94-GHz cloud radar system on a NASA high-altitude ER-2 aircraft. *J. Atmos. Oceanic Technol.,* **21,** 1378–1388.

Long, M. W., 1983: *Radar Reflectivity of Land and Sea.* Artech House, 385 pp.

Mace, G. G., A. J. Heymsfield, and M. R. Poellot, 2002: On retrieving the microphysical properties of cirrus clouds using the moments of the millimeter-wavelength Doppler spectrum. *J. Geophys. Res.,* **107,** 4815, doi:10.1029/2001JD001308.

Majurec, N., S. M. Sekelsky, S. J. Frasier, and S. A. Rutledge, 2005: The advanced multi-frequency radar (AMFR) for remote sensing of clouds and precipitation. Preprints, *32d Conf. on Radar Meteorology,* Albuquerque, NM, Amer. Meteor. Soc., CD-ROM, P1R.6.

Marshall, J. S., and W. McK. Palmer, 1948: The distribution of raindrops with size. *J. Meteor.,* **5,** 165–166.

——, and W. Hitschfeld, 1953: Interpretation of the fluctuating echo from randomly distributed scatterers. *Can. J. Phys.,* **31,** 962–994.

Martner, B. E., R. A. Kropfli, L. E. Ash, and J. B. Snider, 1993: Dual-wavelength differential attenuation radar measurements of cloud liquid water content. *Proc. 26th Conf. on Radar Meteorology,* Norman, OK, Amer. Meteor. Soc., 596–598.

——, and Coauthors, 2002: An overview of NOAA/ETL's scanning Ka-band cloud radar. Preprints, *16th Conf. on Hydrology,* Orlando, FL, Amer. Meteor. Soc., 21–23.

Matrosov, S. Y., 1998: A dual-wavelength radar method to measure snowfall rate. *J. Appl. Meteor.,* **37,** 1510–1521.

——, A. V. Korolev, and A. J. Heymsfield, 2002: Profiling cloud ice mass and particle characteristic size from doppler radar measurements. *J. Atmos. Oceanic Technol.,* **19,** 1003–1018.

McClatchey, R. A., R. W. Fenn, J. E., A. Selby, F. E. Volz, and J. S. Garing, 1972: Optical properties of the atmosphere. 3d ed. Air Force Cambridge Research Labs, Environmental Research Paper AFCRL-72-0497, 108 pp.

Mead, J. B., and K. Widener, 2005: W-band ARM cloud radar. Preprints. *32th Int. Conf. on Radar Meteorology,* Albuquerque, NM, Amer. Meteor. Soc., CD-ROM, P1R.3.

——, A. L. Pazmany, S. M. Sekelsky, and R. E. McIntosh, 1994: Millimeter-wave radar for remotely sensing clouds and precipitation. *Proc. IEEE,* **2,** 1891–1906.

Mie, G., 1908: Beitrage zur Optic truber Medien, speziell kolloidaler Metallosungen. *Ann. Phys.,* **30,** 377–442.

Miller, M. A., and A. Slingo, 2007: The ARM Mobile Facility and its first international deployment: Measuring radiative flux divergence in West Africa. *Bull. Amer. Meteor. Soc.,* **88,** 1225–1244.

——, G. Johannes, V. Craig, G. J. Lehenbauer, J. S. Tongue, and E. E. Clothiaux, 1998: Detection of nonprecipitating clouds with the WSR-88D: A theoretical and experimental survey of capabilities and limitations. *Wea. Forecasting,* **13,** 1046–1062.

Mishchenko, M. I., 2000: Calculations of the amplitude matrix for a nonspherical particle in the fixed orientation. *Appl. Opt.,* **39,** 1026–1031.

——, and L. D. Travis, 1994: T-matrix computations of light scattering by large spheroidal particles. *Opt. Comm.,* **109,** 16–21.

Moran, K. P., B. E. Martner, M. J. Post, R. A. Kropfli, D. C. Welsh, and K. B. Widener, 1998: An unattended cloud-profiling radar for use in climate research. *Bull. Amer. Meteor. Soc.,* **79,** 443–455.

O'Connor, E. J., R. J. Hogan, and A. J. Illingworth, 2005: Retrieving stratocumulus drizzle parameters using Doppler radar and lidar. *J. Appl. Meteor.,* **44,** 14–27.

Pasqualucci, F., B. W. Bartram, R. A. Kropfli, and W. R. Moninger, 1983: A millimeter-wavelength dual-polarization Doppler radar for cloud and precipitation studies. *J. Climate Appl. Meteor.,* **22,** 758–765.

Paulsen, W. H., P. J. Petrocchi, and G. McLean, 1970: Operational utilization of the AN/TPQ-11 cloud detection radar. AFCRL-70-0335, Instrumentation Paper No. 166, 59 pp. [NTIS AD709364.]

Pazmany, A. L., R. E. McIntosh, R. Kelly, and G. Vali, 1994: An airborne 95-GHz dual polarization radar for cloud studies. *IEEE Trans. Geosci. Remote Sens.,* **1,** 731–739.

Petrocchi, R. J., and W. H. Paulsen, 1966: Meteorological significance of vertical density profiles of clouds and precipitation obtained with the An/TPQ-11 radar. *Proc. 12th Radar Meteorology Conf.,* Norman, OK, Amer. Meteor. Soc., 467–474.

Plank, V. G., D. Atlas, and W. H. Paulsen, 1955: The nature and detectability of clouds and precipitation as determined by 1.25 centimeter radar. *J. Meteor.,* **12,** 358–378.

Racette, P. E., G. M. Heymsfield, L. Li, L. Tian and E. Zenker, 2003: The cloud radar system. Preprints, *31st Conf. on Radar Meteorology,* Seattle, WA, Amer. Meteor. Soc., 237–240.

Reehorst, A. L., and G. G. Koenig, 2004: Preliminary analysis of X-band and Ka-band radar for use in the detection of icing conditions aloft. AIAA-2004-0233, NASA/TM—2004-212901, 17 pp.

Reinking, R. F., and Coauthors, 2001: Concept and design of a ground-based remote icing detection system. Preprints, *30th Int. Conf. on Radar Meteorology,* Munich, Germany, Amer. Meteor. Soc., CD-ROM, P5.2.

——, S. Y. Matrosov, R. A. Kropfli, and B. W. Bartram, 2002: Evaluation of a 45° slant quasi-linear radar polarization state for distinguishing drizzle droplets, pristine ice crystals, and less regular ice particles. *J. Atmos. Oceanic Technol.,* **19,** 296–321.

Rogers, R. R., P. L. Smith, 1996: A short history of radar meteorology. *Historical Essays on Meteorology 1919–1995,* J. R. Fleming, Ed., Amer. Meteor. Soc., 57–98.

Sadowy, G., and Coauthors, 1997: The NASA DC-8 airborne cloud radar: Design and preliminary results. *Int. Geosci. Remote Sens. Symp.,* **4,** 1466–1469.

Sassen, K., J. R. Campbell, J. Zhu, P. Kollias, M. D. Shupe, and C. Williams, 2005: Lidar and triple-wavelength Doppler radar measurements of the melting layer: A revised model for dark- and bright band phenomena. *J. Appl. Meteor.,* **44,** 301–312.

Sekelsky, S. M., and R. E. McIntosh, 1996: Cloud observations with polarimetrc 33 GHz and 95 GHz radar. *Meteor. Atmos. Phys.,* **59,** 123–140.

——, W. L. Ecklund, J. M. Firda, K. S. Gage, and R. E. McIntosh, 1999: Particle size estimation in ice-phase clouds using multi-frequency radar reflectivity at 95, 33, and 2.8 GHz. *J. Appl. Meteor.,* **38,** 5–28.

Shupe, M. D., P. Kollias, S. Y. Matrosov, and T. L. Schneider, 2004: Deriving Mixed-Phase Cloud Properties from Doppler Radar Spectra. *J. Atmos. Oceanic Technol.,* **21,** 660–670.

Stephens, G. L., 1994: *Remote Sensing of the Lower Atmosphere: An Introduction.* Oxford University Press, 523 pp.

——, and Coauthors, 2002: The CloudSat Mission and the A-Train: A new dimension of space-based observations of clouds and precipitation. *Bull. Amer. Meteor. Soc.,* **83,** 1771–1790.

Stokes, G. M., and S. E. Schwartz, 1994: The Atmospheric Radiation Measurement (ARM) Program: Programmatic background and design of the Cloud and Radiation Test Bed. *Bull. Amer. Meteor. Soc.,* **75,** 1201–1222.

Vali, G., R. Kelly, A. Pazmany, and R. E. McIntosh, 1995: Airborne radar and in-situ observations of a shallow stratus with drizzle. *Atmos. Res.,* **38,** 361–380.

——, —— J. French, S. Haimov, D. Leon, R. E. McIntosh, and A. Pazmany, 1998: Finescale structure and microphysics of coastal stratus. *J. Atmos. Sci.,* **55,** 3540–3564.

Wang, J., and B. Geerts, 2003: Identifying drizzle within marine stratus with W-band radar reflectivity. *Atmos. Res.,* **69,** 1–27.

Yang, P., and Coauthors, 2003: Enhanced lidar backscattering by quasi-horizontally oriented ice crystal plates in cirrus clouds. *J. Quant. Spectrosc. Radiat. Transfer,* **79–80,** 1139–1157.